Cell. Mol. Life Sci. (2012) 69:651–661
DOI 10.1007/s00018-011-0774-7

Cellular and Molecular Life Sciences

RESEARCH ARTICLE

PRG-1 transcriptional regulation independent from Nex1/Math2-mediated activation

Beate Geist · Brita Vorwerk · Pierluca Coiro · Olaf Ninnemann · Robert Nitsch

Received: 4 April 2011 / Revised: 6 July 2011 / Accepted: 7 July 2011 / Published online: 31 July 2011

Abstract Plasticity-related gene 1 (PRG-1) is a novel player in glutamatergic synaptic transmission, acting by interfering with lysophosphatidic acid (LPA)-dependent signaling pathways. In the central nervous system, PRG-1 expression is restricted to postsynaptic dendrites on glutamatergic neurons. In this study, we describe the promoter architecture of the PRG-1 gene using RNA ligase-mediated rapid amplification of cDNA ends (RLM-Race) and PCR analysis. We found that PRG-1 expression is under the control of a TATA-less promoter with multiple transcription start sites. We demonstrated also that 200-kb genomic environment of the PRG-1 gene is sufficient to mediate cell type-specific expression in a reporter mouse model. Characterization of the PRG-1 promoter resulted in the identification of a 450-bp sequence, mediating $\approx$40-fold enhancement of transcription in cultured primary neurons compared to controls, and which induced reporter expression in slice cultures in neurons. Recently, the regulation of PRG-1 by the basic helix-loop-helix transcription factor Nex1 (Math2, NeuroD6) was reported. However, our studies in Nex1-null-mice revealed that Nex1-deficiency induces no change in PRG-1 expression and localization. We detected an additional Nex1-independent regulation mechanism that increases PRG-1 expression and mediates neuron-specific expression in an organotypic environment.

Keywords TATA-less promoter · Basic helix-loop-helix transcription factor · Dual-luciferase assay · RLM-Race

Introduction

Plasticity related genes (PRGs), notably PRG-1 and PRG-3, act in a variety of neuronal processes like filopodia formation, neurite extension, axonal path finding, and reorganization after lesions [5, 25, 27, 32]. PRG-1 is vertebrate-specific, most prominently expressed in the CNS. At embryonic day 19 (E19), the mRNA is detected in the subventricular zone and hippocampal anlage. After birth, PRG-1 transcripts are strongly upregulated in the entire brain, especially in the hippocampus and entorhinal cortex [4], and the protein is found exclusively on glutamatergic neurons in the CNS. Recently, analysis of PRG-1 null mouse models elucidated the modulatory role of the postsynaptically localized PRG-1 protein during excitatory synaptic transmission on glutamatergic neurons. This role of PRG-1 in neuronal transmission is thought to depend on an interaction of PRG-1 and lipid phosphates like LPA, acting through presynaptic LPA_2-receptors [34]. In order to elucidate the peculiar expression profile of PRG-1 in neurons, we generated a reporter mouse model expressing YPF controlled by

Electronic supplementary material The online version of this article (doi:10.1007/s00018-011-0774-7) contains supplementary material, which is available to authorized users.

B. Geist · R. Nitsch (✉)
Institute for Microanatomy and Neurobiology,
University Medical Center, Johannes Gutenberg University
Mainz, 55131 Mainz, Germany
e-mail: robert.nitsch@unimedizin-mainz.de

B. Vorwerk · P. Coiro · O. Ninnemann
Institute of Cell Biology and Neurobiology, Center for Anatomy,
Charité, Universitätsmedizin Berlin, Charitéplatz 1,
10117 Berlin, Germany

Present Address:
B. Geist
Institute of Cell Biology and Neurobiology, Center for Anatomy,
Charité, Universitätsmedizin Berlin, Charitéplatz 1,
10117 Berlin, Germany

the native PRG-1 promoter and were able to show that 200-kb sequence enclosing the PRG-1 gene are effectual to confer cell type-specific expression. We also performed RLM-Race and mapped additional transcription start points (TSS) in rodents and confirmed these via PCR-analysis.

A recent study displayed the influence of Nex1, a homolog of the *Drosophila* proneural gene *atonal* belonging to the family of basic helix-loop-helix (bHLH) transcription factors, on PRG-1 expression. bHLH transcription factors bind to the consensus sequence CANNTG (designated as E-box), located in a variety of promoter and enhancer elements [20]. Nex1 expression is CNS specific, prominent in pyramidal neurons, dentate gyrus, and mossy and granule cells [9]. Expression starts at embryonic day 12 [30] and peaks in the first postnatal week parallel to dendritic arborization and synaptogenesis of cortical neurons [3]. Expression is sustained in mature neocortical and hippocampal pyramidal neurons, in mature neurons of the entorhinal cortex, subicular cortex, cingulate gyrus, amygdala, and cerebellum [29]. Besides its pattern of expression, knowledge of Nex1 functions in vivo is limited, as Nex1-null-mice studies failed to show a distinct phenotype, probably due to functional redundancy of bHLH transcription factors. Studies in cell-culture models suggested several functions for Nex1 that might be relevant for neurogenesis, neuronal differentiation, and cellular maintenance. Constitutive over-expression of Nex1 induces spontaneous neuritogenesis, promotes neurite outgrowth and regeneration in PC 12 cells [37, 38]. In vitro, Nex1 regulates a molecular chaperone network through the expression of heat shock proteins and connects neuronal differentiation with survival pathways [36]. To determine the regulatory role of Nex1 in PRG-1 expression, we performed dual-luciferase assays in primary cultured cells and analyzed elements displaying transcriptional activation regarding Nex1 regulation. To further characterize Nex1-dependent PRG-1 regulation, we determined PRG-1 expression and localization in Nex1-null mice.

Materials and methods

PRG-1-YFP-BAC-reporter mouse

Via recombination processes, we inserted the sequence of cytoplasmic yellow fluorescent protein (YFP) reporter into the translation start point of the PRG-1 gene, located on the bacterial artificial chromosome (BAC) RP 23-340J18, accession (start/end): AQ976872, AQ976874 in pBACe3.6 (RZPD, Berlin, Germany). The sequence of YFP was inserted into the translation start site of PRG-1 as described in detail (http://www.gensat.org/BACProtocol.pdf). Linearized BAC-DNA was microinjected into zygotes of NMRI-foster mice at the Max Delbrück Centrum (Berlin, Germany). PRG-1 KO-mouse: Generation described in detail [34]. Nex1 KO-mouse was kindly provided by Nave [28].

Messenger RNA isolation

mRNA from C57/Bl6 mice (P30) was isolated via μMacs (Miltenyi Biotec, Bergisch Gladbach, Germany) according to the manufacturer's recommendations.

RNA-ligase-mediated rapid amplification of cDNA ends (RLM-Race)

mRNA (250 ng sample) obtained from P30 mouse brain (C57/Bl6), were processed for RLM-Race using the GeneRacer™-kit (Invitrogen, Carlsbad, CA, USA) according to the manufacturer's recommendations. PCR amplification was performed first with the GeneRacer 5′Primer and the PRG-1 specific 3′-Primers, Rat: R1 5′aacctgtgcactcc ggattcagttgcta-3′, R2 5′-gtgatcaaggacagcgtcaccctcctg-3, R3 5′-gcggtggagagcccagggagagtggca-3′; Mouse: M1 5′-atctg tgggatcatctgcggactaacac-3, M2 5′-tttgccgctgtgtatgtgtccatg tact-3′, M3 5′-gtcttagcatgccgtacattgagccaac-3′. Amplified fragments were inserted into the plasmid PCR2.1-TOPO (Invitrogen, Carlsbad, CA, USA) and *E. coli* (XL1-Blue) were transformed. Subsequently, positive clones were sequenced.

Primary cell culture

Primary hippocampal neurons were prepared from embryonic day 17(E17) C57/Bl6 mouse pubs or from E18 Wistar rat pubs as described [1, 2]. The cells were cultured at a density of 50,000 cells/cm^2 on poly-L-lysine coated polystyrene multiwell plates (Becton–Dickinson Labware, Le Pont De Claix, France) in Neurobasal A medium supplemented with 2% B27 (Invitrogen, Carlsbad, CA, USA), 0.5 mM glutamine [6], and the antibiotics penicillin and streptomycin. Primary cortical astrocytes were prepared from postnatal day 2 (P2) C57/Bl6 mouse pubs as described [17].

Vector construction

To generate promoter deletion constructs, we amplified specific-length fragments from the human, mouse and rat PRG-1 promoter with Herculase (Stratagene, La Jolla, CA, USA). Amplified fragments were restricted and inserted into pGL3basic (Promega, Madison, WI, USA). Denomination of vectors referred to the position of the inserted region in relation to the translation start point, ATG. The coding sequence of Nex1 was inserted into pCMV-HA (Clontech, Takara Bio Europe, Saint-Germain-en-Laye, France).

Transient transfection and dual-luciferase assay

All cells were transiently transfected with equal amounts of the various luciferase-fusion constructs or pGL3basic in serum-free growth media using transfection reagents according to the manufacturer's protocol. pHRLtK (Promega, Madison, WI, USA) containing the *Renilla* luciferase gene fused to the herpes simplex virus thymidin kinase promoter was cotransfected in order to normalize transfection efficiencies. HEK 293 cells (ATCC, Manassas, VA, USA) were transfected with Fugene6-reagent (Roche, Mannheim, Germany). Primary neurons and astrocytes were transfected with Effectene (Qiagen, Hilden, Germany). The cells were lysed 48 h after transfection and the luciferase activities of the cell lysates were determined using the dual-luciferase reporter assay system (Promega, Madison, WI, USA). Transfections with each construct were performed at least three times.

cDNA synthesis

mRNA was digested with DNase (Roche, Mannheim, Germany) prior to cDNA synthesis. cDNA was synthesized with random hexamer primers and Superscript™ III RT (Invitrogen, Carlsbad, CA, USA) according to the manufacturer's recommendations.

PCR analysis

PCR amplification of cDNAs was performed at an annealing temperature of 59°C in 34 cycles. Negative controls with *A. bidest* as template showed no amplification.

Primers: m1fw: 5′ -gctgctatcccttgcccgcaaaacac-3′, m2fw: 5′ -cctatttttgacgtcaagctcaacc-3′, m3fw: 5′- ggcagggctgt cacgcttgggtagc-3′, mrev: 5′- caacgaaataaaaacagggcag-3′. Amplificates were separated in 2% (w/v) ethidiumbromide stained agarose gels.

Slice culture and cell labeling by electroporation

Mice (C57/Bl6) at postnatal day 5 (P5) were used for the organotypic slice culture techniques, as described previously [41, 42]. In brief, 300-µm coronal cortical slices with hippocampal commissure were cultured in six-well plates on 0.4-µm Millicell Inserts (Millicell-CM PICMORG 50, Millipore) floating on 1-ml culture medium (50% Dubecco's minimal essential medium, 25% heat-inactivated horse serum, 25% Hank's balanced salt solution, 6.5 mg/ml glucose and 100 U/ml streptomycin and penicillin). The cultures were incubated in 5% CO_2 at 37°C. The hippocampal CA3 region of P5 cortical slices were injected with reporter-plasmid containing solution. We used plasmids in a concentration of 2 µg/µl for the local electroporation technique, as described previously [35]. The electroporation (100 V, pulse duration, 5 ms, interval 500 ms, two times) was performed 1 h after slice preparation. The electroporated postnatal slices were incubated for 2 days in 5% CO_2 at 37°C. Multiple sequence alignment: ClustalW: http://www.ebi.ac.uk/Tools/clustalw2/index.html. Prediction of transcription factor binding sites: AliBaba2.1(gene-regulation.com). Prediction of CpG islands: http://cpgislands.usc.edu/.

Electrophoretic mobility shift assays

Nuclear protein extracts from primary cortical rat neurons were prepared and electrophoretic mobility shift assays were performed exactly as described [18]. The sequence of the oligonucleotides used were as follows (sense strand): EMSA1 5′-ccttggctcctcagccttgcttctgcaga-3′; EMSA2 5′-agaaaccaggagtgcctcccccactatt-3′; EMSA3 5′-tatttttgacgtcaagctcagacaacca-3′; EMSA4 5′-accagcagaggagcctcacagcttgg-3′; EMSA5 5′-gcttgggcggtggagagcccagggagagt-3′; SP1 5′-attcgatcggggcggggcgag-3′; CREB 5′-agagattgcctgacgtcagagagctag-3′.

Tissue preparation and Western blot

All procedures involving animals were performed in accordance with the European Community′s Council Directive of 24th November 1986 (86/609/EEC). The animals were killed and their brains were removed and homogenized with an ULTRA-TURRAX® homogenizer in STM-buffer: 250 mM sucrose, 10 mM Tris, 1 mM $MgCl_2$ with 1% Triton (v/v) and a proteinase inhibitor cocktail (Sigma, St. Louis, MO, USA). Proteins were electrophoresed in 10% polyacrylamide-sodium dodecyl sulfate gels and electrotransferred to nitrocellulose membranes (Schleicher & Schuell, Dassel, Germany). The blots were incubated with either rabbit polyclonal antibody against PRG-1(1:1,000; generated in our lab), rabbit polyclonal antibody against Nex1/Math2 (1:1,000; Millipore, Schwalbach, Germany), or a mouse monoclonal antibody against β-Actin (1:5,000, Sigma, St. Louis, MO, USA). After washing five times with PBS, the blots were incubated with horse radish peroxidase-conjugated secondary antibody, treated with chemiluminescence reagents (GE Healthcare, Munich, Germany), and exposed to x-ray films. If reprobing was necessary, nitrocellulose membranes were stripped with 100 mM sodium citrate.

Immunohistochemistry

Horizontal brain sections of mouse brains (50 µm) were fixed by perfusion with 4% PFA, and sections of hippocampal slices (100 µm) were fixed 30 min with 4% PFA. Sections were processed for immunostaining using a rabbit

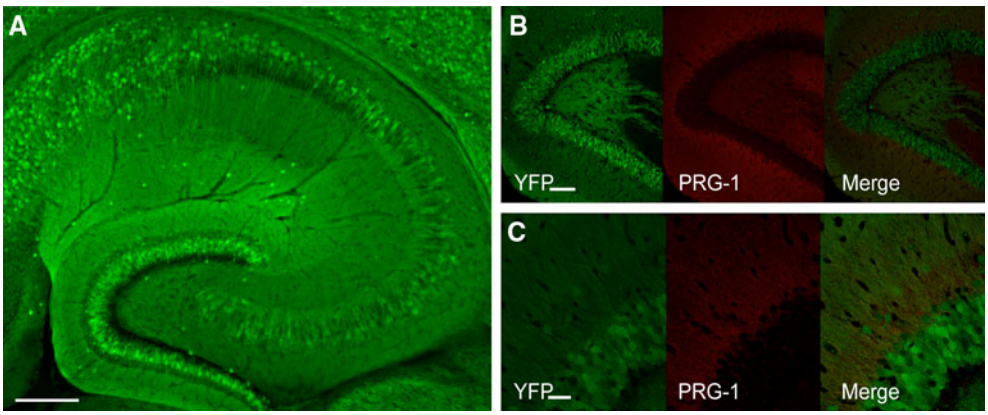

Fig. 1 Yellow fluorescent protein expression under control of the PRG-1 promoter. **a** Hippocampal section of an adult (P30) PRG-1-Bac-YFP reporter mouse, axons, and cell bodies of PRG-1-expressing neurons are labeled by the cytoplasmic reporter protein. The strongest fluorescence was detected in the granular cell layer and CA1-CA3 pyramidal cell layer, *Scale bar* = 200 μm. **b** PRG-1 expression in the dentate gyrus of an adult (P30) PRG-1-Bac-YFP reporter mouse. Dendrites of PRG-1-expressing cells are labeled by PRG-1 antibody and the corresponding cell bodies are labeled by YFP expression, *Scale bar* = 100 μm. **c** PRG-1 expression in the granule cell layer of an adult (P30) PRG-1-Bac-YFP reporter mouse, *Scale bar* = 15 μm

polyclonal antibody against PRG-1 (1:1,000), a chicken polyclonal antibody against *β*-galactosidase (1:2,000, abcam, Cambridge, MA, USA), a rabbit polyclonal antibody against parvalbumin (1:2,500, Swant, Bellinzona, Switzerland), calretinin (1:1,000, Swant, Bellinzona, Switzerland), NeuN (1:1,000, Chemicon, Temecula, USA), and GFP (1:1,000, abcam, Cambridge, USA). To suppress non-specific binding, sections were incubated in 0.01 M PBS, 5% serum and 0.01% Triton X-100, for 1 h at RT. Thereafter, sections were incubated with primary antibody overnight at 4°C. After washing, sections were incubated with a secondary fluorochrome-conjugated antibody (1:2,000; Alexa Fluor 568/Alexa Fluor 488; Molecular Probes, Eugene, OR, USA). The specificity of the antibody was tested by omitting the primary antibody or by replacing it with an equivalent concentration of non-specific IgG. No unspecific immunostaining was detected. Confocal images were obtained with a LEICA LCS SL confocal microscope (Leica Microsystems GmbH, Wetzlar, Germany). Fluorescent images were obtained with an Olympus BX 50 microscope. Subsequent montage of multiple images to overview screens was done using MetaMorph software (Downingtown, PA, USA).

Results

200-kb genomic sequence enclosing PRG-1 is sufficient to confer PRG-1-specific, strictly neuronal, and neuronal subtype-specific expression pattern in a reporter mouse line

To assess the promoter region necessary for proper PRG-1 expression, we created a reporter mouse that expressed yellow fluorescent protein (YFP) under the control of native PRG-1 promoter elements in 200-kb genomic sequence surrounding the *prg-1* gene. We characterized three independent lines containing the full-length transgene sequence. We found identical spatial and temporal, exclusively neuronal expression of the YFP-reporter protein in all examined lines. The strength of fluorescence varied within the three lines, corresponding to different copy numbers of the inserted transgene in the three different transgenic lines, investigated via Southern blot (data not shown). Adult (P30) animals showed strong signals in hippocampal principal neurons of a PRG-1-YFP-BAC-mouse (Fig. 1a). Dendrites of PRG-1-expressing neurons were labeled with PRG-1 antibody; corresponding cell bodies were labeled by expression of yellow fluorescent protein (Fig. 1b, c).

PRG-1 protein-containing cells expressed YFP, but in some PRG-1-positive cells reporter gene expression was minimal or missing. Correct reporter gene expression was confirmed via colocalization studies with PRG-1-YFP-BAC-mice crossbred with PRG-1-null mice harboring a *β*-galactosidase reporter cassette under control of the PRG-1 promoter. Heterozygous offspring was analyzed via immunochemistry (Supplemental Fig. 1A–C) by comparing the cytoplasmic reporters yellow fluorescent protein and *β*-galactosidase. Immunocytochemistry for parvalbumin and calretinin (Fig. 2a, b) confirmed no colocalization with interneurons, as described previously for PRG-1 [34]. This indicates that all necessary elements for neuronal subtype expression of *prg-1* are present on the BAC sequence selected for transgene generation. In addition, no misexpression of the reporter gene in all animals analyzed was observed. The selected 200-kb genomic environment of the *PRG-1* gene was adequate to mediate cell type-specific expression, independent of transgene insertion loci.

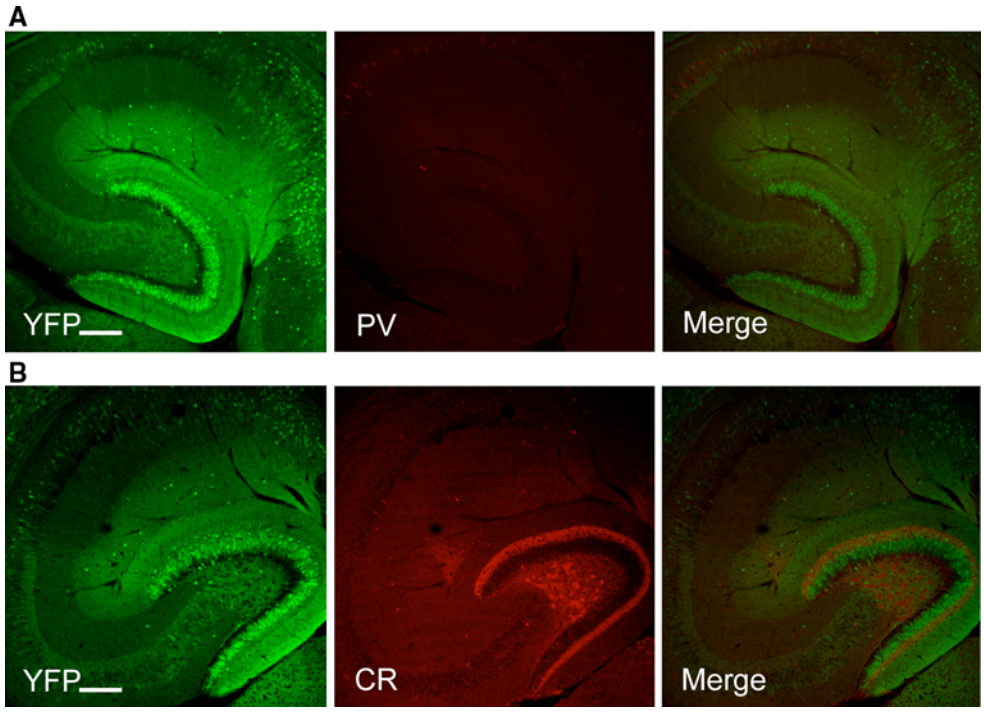

Fig. 2 Immuno-colocalization confirms accurate reporter gene expression in PRG-1-YFP-BAC reporter mice (P30). PRG-1-YFP-BAC mice display no reporter gene expression in interneurons, indicating neuronal subtype-specific expression of the reporter gene. Immunostaining for **a** parvalbumin and **B** calretinin, *scale bar* = 200 µm

Identification of multiple transcription start sites (TSS) for PRG-1 in rodents

We performed RLM-Race to specifically detect capped transcripts and mapped several TSS in rat and mouse. Rat transcripts start at position: −201, −160, −156, −96, +46, +69 given in relation to the translation start point ATG = + 1. Mouse transcripts were mapped at position: −149, −144, −101, +2, +43, +45, +71 and +79 (Fig. 3a). Some TSS were located downstream of the first translation start point, revealing a second putative translation start site, which is conserved in the mammalian PRG-1 sequences. In mouse and rat sequences, the second ATG was located at position +148, and in human at position +145. Neither the TSS identified initially (NM_001001508) nor the other TSS in the same distance to the translation start site, could be mapped in this analysis. To confirm the initially identified TSS, we performed PCR analysis of murine cDNAs. We used the following primer combinations for amplification of sequence elements with subsequent denoted position in relation to the first ATG: m1: −119fw/+ 222rev; m2: −240fw/+ 222rev; m3: −509fw/+ 222rev (Fig. 3b). The PCR analysis confirmed the existence of transcripts with similar length as the originally identified PRG-1 TSS in rat (Fig. 3c). Long amplificates corresponding to the initially identified rat TSS occur to a lesser extent than amplificates corresponding to TSS identified in this study (one selective figure of five independent experiments shown). With increasing distance to the first ATG, the amount of amplified transcript decreases, thus indicating m1 as the main transcript. Positive controls with murine genomic DNA as template documented that the small amounts of amplificate with primer combination m3 are not a result of differences in PCR efficiency.

A 450-bp sequence element of the human and rodent PRG-1 promoter is sufficient to stimulate neuronal transcription

To further characterize the promoter architecture of PRG-1, we searched for sequence elements responsible for specific neuronal expression of PRG-1. We performed dual-luciferase-assays with several deletion-constructs of the PRG-1 promoter in primary neurons and astrocytes. Transfection of human PRG-1 promoter deletion-constructs in primary rat neurons and astrocytes resulted in identification of a 450-bp sequence (h−300/+143), mediating ≈40-fold enhancement of transcription in primary rat neurons compared to control (Fig. 4a). Truncation of this fragment to 300 bp (h−169/+143) leads to a 50% reduction of specificity for neuronal transcription down to the level of stimulation in astrocytes. Transfection of this 300-bp sequence in reverse orientation (h+143/−169) leads to almost complete loss of transcriptional activity. All

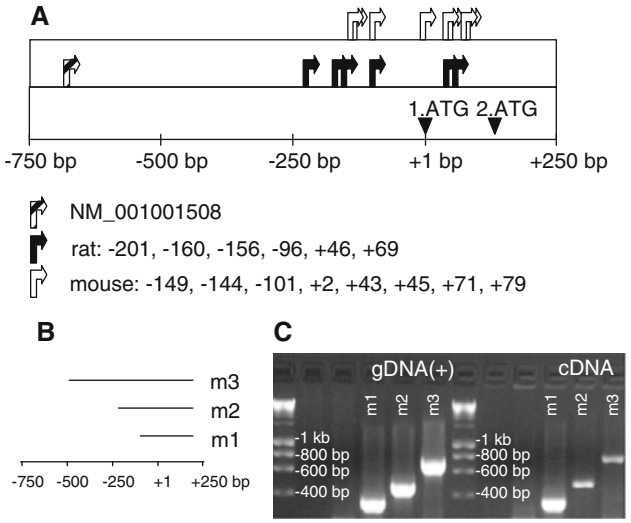

Fig. 3 **a** PRG-1 is transcribed from multiple transcription start points in rodents. Mapped transcription start sites of PRG-1 in rat (*filled arrows*): −201, −160, −156, −96, +46, and +69. The positions are designated in relation to the first translation start site (ATG = +1). Mapped transcription start sites in mouse (*open arrows*): −149, −144, −101, +2, +43, +45, +71, and +79. A second putative translation start site is conserved in mammals, in mouse and rat at position +145 and in the human sequence at position +143. To affirmate transcripts with 5′- extension according to NM_001001508, we amplified corresponding sequences with following primer pairs: m1: −119/+222; m2: −240/+ 222; m3: −509/+ 222. **b** Position of amplificates in relation to the first murine ATG. **c** Positive control amplified from murine genomic DNA (gDNA) for comparison of amplification efficacy. PCR products were amplified from murine cDNA

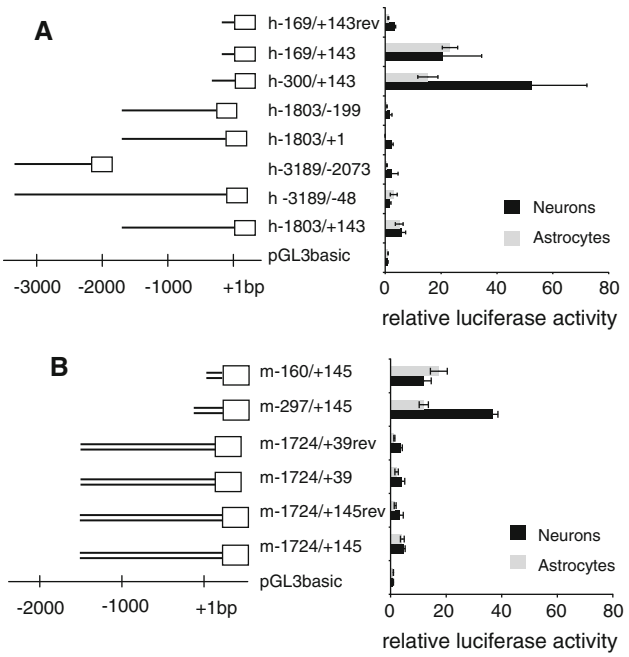

Fig. 4 Identification of a sequence element in the human and murine PRG-1 promoter sufficient to confer neuronal transcription. **a** Human PRG-1 promoter 5′end deletion constructs were ligated in the dual-luciferase reporter gene vector pGL3. Constructs and expression control pHRLtk (Promega) were co-transfected in primary rat neurons and astrocytes. The left side of the figure shows the position of the transfected construct in relation to the first translation start site (ATG = +1) of PRG-1. Additionally, the nomenclature of the constructs refers to their exact location in relation to the first translation start site. The right side of the figure displays the relative luciferase activity of the transfected constructs. The relative luciferase activity is defined as the ratio of Firefly luciferase activity versus Renilla luciferase activity. Basal-level luciferase activity of cells transfected with pGL3basic and pHRLtk (Promega) was taken as 1%. Results are expressed as fold increase ±SD. The experiments were repeated at least three times independently. **b** Murine PRG-1/pGL3 reporter constructs and expression control pHRLtk were co-transfected in primary mouse neurons and astrocytes

constructs with a 3′-extension to the second putative translation start site display enhanced transcriptional activity compared to controls.

The homologous 450-bp sequences of the murine promoter region (m−297/+145) induce similar transcriptional progression in primary mouse neurons compared to astrocytes (Fig. 4b). Truncation to a homologous murine 300-bp sequence (m−160/+145) induces the same effect in the homologous system as in the previously mentioned heterologous system. Transfection of other murine PRG-1 promoter constructs failed to identify other sequence fragments with similar transcriptional activity in primary mouse neurons. Interestingly, the addition of 5′-sequences to the 450-bp minimal promoter led to a strong decrease of transcriptional activity.

The 450-bp minimal promoter confers neuronal expression in organotypic slice cultures

To investigate if the identified 450-bp promoter fragment is effectual under in vivo conditions, we electroporated this construct in P5 hippocampal slices. We exchanged the luciferase reporter sequence with the sequence of GFP in the 450-bp pGl3 promoter construct used in the dual-luciferase assays. Expression of GFP was detected, which confirms the functionality of this promoter in brain tissue (Fig. 5). Immunohistochemical analysis by NeuN antibody colabeling documented GFP expression to occur in neurons.

Neuronal transcription of PRG-1 is stimulated independently from Nex1

For analysis of Nex1 effects as reported by [40], all tested PRG-1 promoter-deletion constructs used in this study were cotransfected with Nex1 expression vector or control in HEK 293 cells. Nex1 exhibits a minimal stimulation on all tested fragments (Fig. 6a). In contrast to primary cell studies, the 300-bp Fragment (h−169/F+143; m−160/+145) of the human and mouse PRG-1 promoter showed

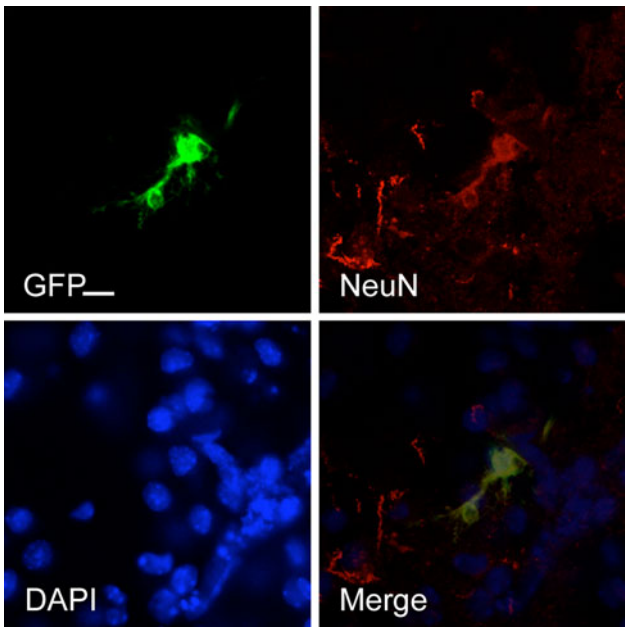

Fig. 5 The 450-bp minimal promoter mediates neuronal expression of GFP. Hippocampal slices of P5 mice electroporated with the 450-bp minimal promoter driving GFP expression. Labeling with the neuronal marker NeuN reveals strict neuronal expression of the reporter, *scale bar* = 10 μm

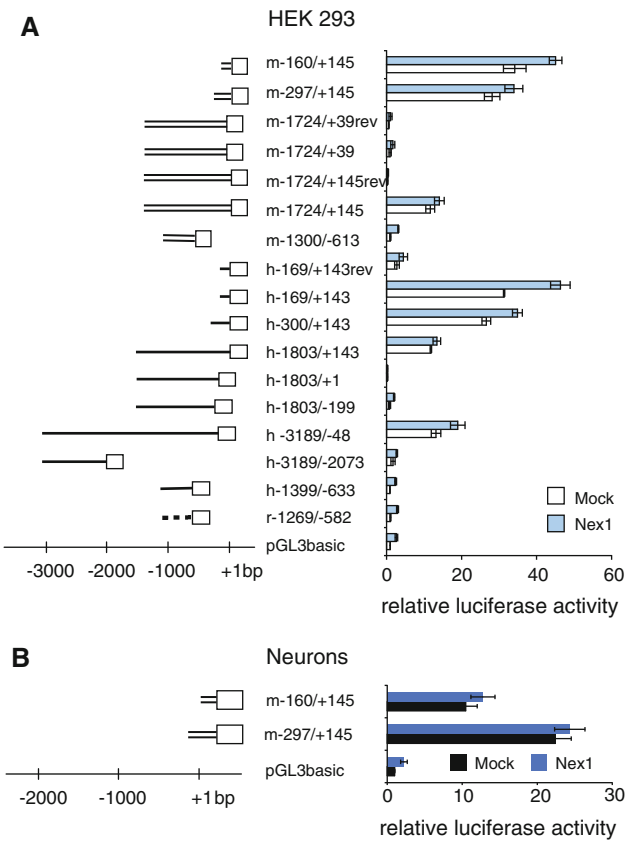

Fig. 6 Nex1 stimulates general transcription from PRG-1 promoter deletion constructs. **a** All PRG-1/pGL3 reporter constructs, expression control pHRLtk (Promega), and a Nex1 expression vector or mock were co-transfected in HEK293 cells. The left side of the figure shows the position of the transfected construct in relation to the first translation start site (ATG = +1) of PRG-1. Additionally, the nomenclature of the constructs refers to their exact location in relation to the first translation start site. The right side of the figure displays the relative luciferase activity of the transfected constructs. The relative luciferase activity is defined as the ratio of Firefly luciferase activity versus Renilla luciferase activity. Basal-level luciferase activity of cells transfected with pGL3basic and pHRLtk (Promega) was taken as 1%. Results are expressed as fold increase ±SD. The experiments were repeated at least three times independently. Control vectors: h−1399/−633, m−1300/−613, r−1269/−582 were transfected for monitoring Nex1-dependent activation. **b** The murine luciferase reporter constructs (450/300 bp) displaying the strongest specific neuronal transcriptional activities, expression control of pHRLtk, and a Math2/Nex1 expression vector or mock were co-transfected in primary mouse neurons. Only a minimal effect of Nex1 coexpression is seen

the highest rate of activity in HEK 293 cells instead of the 450-bp minimal promoter (h−300/+143; m−297/+145). Interestingly, the mouse 300-bp fragment contains no functional E-Box motif.

The region of the rat PRG-1 promoter (−1,269 to −582 bp relative to the first ATG = +1) where binding of Nex1 to an E-box motif was documented via chromatin immunoprecipitation and which displays the strongest Nex1-dependent stimulation [40], was subcloned in pGL3. The homologous regions of mouse and human sequences (m−1300/−613, h−1399/−613) were also subcloned as controls. Rodent-positive controls exhibit similar expression stimulation following Nex1 cotransfection, as published.

The empty vector pGL3 differs in transcriptional activation by Nex1 from the vector pGL4 used in the aforementioned study, hence influences resulting by the usage of different vector backbones could not be excluded. Furthermore, the human positive control without conserved E-Box motifs (Supplemental Fig. 2) at the positions found in the rodent sequences displays similar enhancement of reporter expression. The 450- and 300-bp fragments showing the highest activity have not been analyzed in earlier studies.

To further analyze Nex1 effects on the 450- and 300-bp sequence elements, murine constructs were cotransfected with a Nex1 expression vector or control in neurons (Fig. 6b). Only minimal increment of transcription could be determined in neurons with the 450- and 300-bp constructs, implicating a Nex1-independent control mechanism.

Further investigation of the 450-bp minimal promoter by electrophoretic mobility shift assays (EMSA)

We have shown in dual-luciferase assays that truncation of the first 150 bp in the human and mouse minimal promoter leads to loss of specific transcriptional stimulation in neurons.

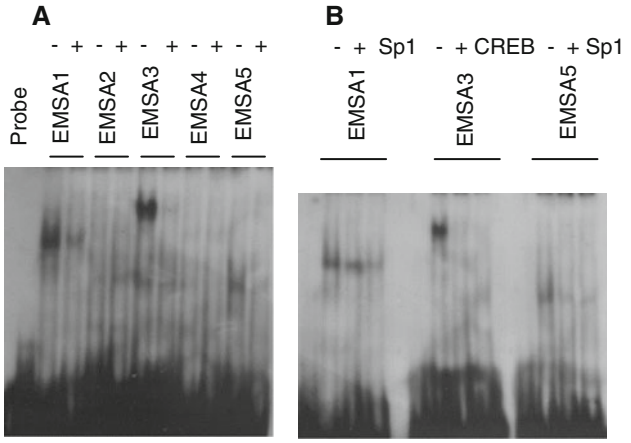

Fig. 7 Electrophoretic mobility shift assays showing the binding of proteins in nuclear extracts of primary rat neurons to oligonucleotide probes representing the 5′portion of the identified minimal promotor. **a** Nuclear extracts were incubated with overlapping oligonucleotide probes (EMSA 1–5) corresponding to a region of 150 bp of the rat minimal promoter sequence, in the absence (−) or presence (+) of a competing unlabeled oligonucleotide of identical probe sequence used in 100-fold excess. **b** Identified DNA–protein complexes were competed with consensus unlabeled SP1 or CREB oligonucleotides due to prediction of transcription factor binding sites on the respective probe

Therefore we investigated binding of transcription factors via EMSA with crude nuclei extracts of cultivated primary rat neurons on five overlapping double-stranded oligonucleotides comprising these 150 bp of the rat sequence. We could detect DNA–protein complexes with the labeled probes EMSA1, EMSA3, and EMSA5 (Fig. 7a). These complexes were competed with 100-fold excess of the respective unlabeled probe. Shifted bands without competition after addition of unlabeled probe were considered as nonspecific binding. Subsequent in silico search for transcription factors predicted binding sites for Sp1 (EMSA1, EMSA5) and CRE (EMSA3) conserved in rodent and human sequences. On that account, we performed gel shifts with the labeled probes EMSA1 and EMSA5 and competed with the respective unlabeled oligonucleotides or an unlabeled oligonucleotide with the Sp1 consensus binding sequence. In case of EMSA3, we competed with an unlabeled oligonucleotide harboring the CREB (cAMP-responsive element binding protein) consensus binding sequence (Fig. 7b). A reduction of the EMSA1-DNA–protein complex was observed after competition with 100-fold excess SP1 oligonucleotide. The EMSA3-DNA–protein complex was competed by 100-fold excess CREB oligonucleotide. The EMSA5-DNA–protein complex was also competed by 100-fold excess SP1 oligonucleotide.

Nex1 deficiency in vivo has no influence on PRG-1 expression

To investigate the influence of Nex1 regulation on PRG-1, we performed Western-blot analysis in Nex1-null mice.

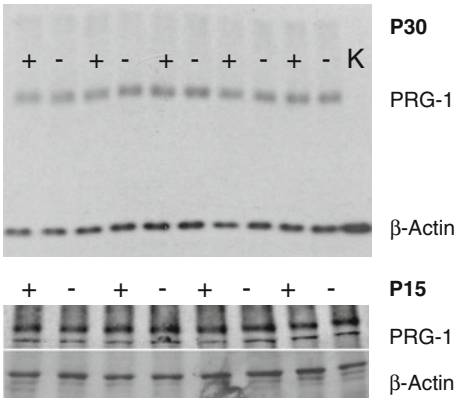

Fig. 8 PRG-1 displays similar expression in adult cortex homogenates (P30) and at the expression maximum at P15. Western-blot analysis of Nex1-null mice (−) and wild-type controls (+), *β*-actin as loading control. For verification of PRG-1 antibody specificity, equal amount of PRG-1KO (K) homogenate was loaded

Cortex homogenates of adult mice (P30) showed unchanged PRG-1 expression in Nex1-null mice compared to controls (Fig. 8). Additional analysis of P15 animals confirmed unchanged PRG-1 levels at the timepoint of highest PRG-1 expression in Nex1-null mice. Western-blot analysis of cortex homogenates of adult (P30) PRG-1-null mice documented unchanged Nex1 expression in PRG-1-null mice compared to controls, implicating no feedback regulation of Nex1 by PRG-1 (Supplemental Fig. 3).

We investigated possible alterations in PRG-1 localization by immunohistochemical analysis via PRG-1 antibody labeling. The dendritic staining showed no difference between adult (P30) Nex1-null mice and controls (data not shown). To compare the amount and position of cell bodies and axons of PRG-1-expressing cells, Nex-null mice were crossed with the PRG-1-YFP-BAC- reporter strain. The amount and localization of the reporter YFP are equal in Nex1-null mice compared to controls (Fig. 9).

Discussion

Our analysis of PRG-1 transcriptional regulation has shown that all regulatory elements for PRG-1-specific gene expression are coded on a 200-kb BAC containing 41-kb PRG-1 genomic sequence, and 64-kb upstream as well as 94-kb downstream sequence. Further, we showed that PRG-1 transcription is initiated at multiple transcription start sites. We detected one sequence element 5′ at the translation start site ATG that mediates specific neuronal transcription in the human and rodent PRG-1 promoter. Although Nex1 stimulated transcription from various putative 5′ PRG-1 promoter fragments, it appears that Nex1 deficiency has no influence on PRG-1 expression in vivo.

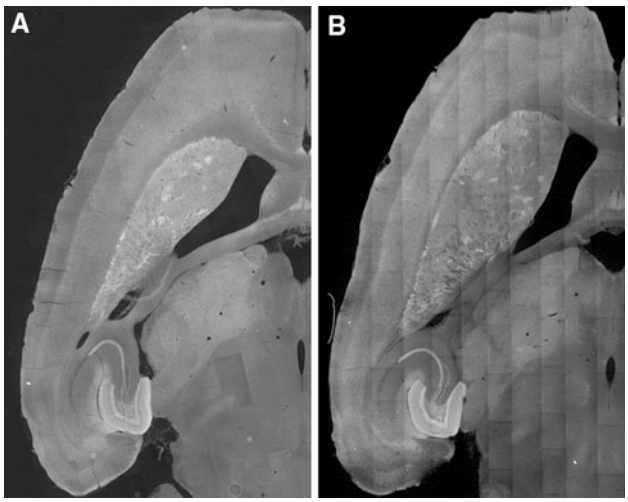

Fig. 9 Unchanged YFP expression in PRG-1-Bac-YFP/Nex1−/− mice. In the PRG-1-Bac-YFP reporter mouse, axons and cell bodies of PRG-1 expressing neurons are labeled by the cytoplasmic reporter protein. Nex1-deficient PRG-1-Bac-YFP reporter mice (**a**) display identical YFP expression to controls (**b**)

PRG-1 belongs to the family of plasticity related genes that possesses homology to lipid phosphate phosphatases and is part of the superfamily of lipid phosphate phosphatases/phosphotransferases [31]. However, PRG-1 shows no enzymatic activity for dephosphorylation of the superfamily-specific substrates such as phosphatidate, lysophosphatidate, or sphingosine-1-phosphate [8], which is due to amino acid exchanges in the catalytic motif that is shared by active PAP-2 family members [7, 22]. PRG-1 is involved in modulation of neuronal transmission via bioactive lipids, such as LPA acting via presynaptic LPA_2 receptors, which are controlled by PRG-1 from the postsynaptic side (specifically at the glutamatergic junction). According to recent data, this action may be mediated by PRG-1 by depleting the pool of bioactive lipids that act on the presynaptic LPA_2 receptors [34].

PRG-1 is transcribed via a type "null" core promoter containing neither TATA box nor initiator element. Multiple start sites are common for this promoter type [24]. The existence of transcription start sites downstream of the first ATG of PRG-1 implies the existence of a second, alternative N-terminus. Beside the full-length protein, the existence of a shorter form, lacking the N-terminal 49 amino acids translated from second ATG, needs to be confirmed. The shorter form of PRG-1 resembles the homologous protein PRG-2 at the N-terminus [5], which is expressed prenatally and has a different expression pattern compared to PRG-1. Thus, it is possible that the short form of PRG-1 substitutes the function of PRG-2 postnatally. Analysis of expressed sequence tag databases revealed the existence of diverse PRGs in all vertebrates examined, but the full-length long form with the additional 49 amino acids at the N-term of PRG-1 could only be found in mammals according to in silico analysis of GenBank sequences. However, a functional role of this N-terminal elongation restricted to mammals remains to be elucidated.

In our present study, expression analysis of the PRG-1-YFP-Bac mouse showed that the chosen BAC sequence is effectual for mediating strict neuronal expression. The peculiar specific neuronal expression of PRG-1 is not mediated via binding of RE I silencing transcription factor (*REST/NRSF*), which was evidenced by the fact that in silico analysis documented the absence of *REST/NRSF*-binding sites on the chosen BAC sequence. To elucidate the transcriptional regulation of PRG-1, we searched for elements responsible for neuronal expression in the putative promoter region. We identified a 450-bp minimal promoter conferring enhanced specific transcription in neurons and electroporation of hippocampal slices documented the capacity of the 450-bp promoter to mediate neuronal expression of a reporter gene.

We have shown in dual-luciferase assays that truncation of 150 bp of the identified minimal promoter leads to reduction of transcriptional stimulation in neurons. Therefore we analyzed this 150-bp sequence via EMSA for competence of protein binding. Analysis of transcription factor binding sites revealed conserved binding sites for Sp1 and CRE (cAMP-responsive element) in the rodent and human sequences. Subsequent EMSA showed that competition with the respective consensus-binding sites against Sp1 and CREB diminish DNA–protein complexes. Sp1 is a ubiquitously expressed transcription factor implicated in transcription of many TATA-less promoters [39]. On that account, it is very unlikely that the specific neuronal stimulation of transcription is mediated by this factor. The cAMP-responsive element binding protein (CREB) is a nuclear protein that modulates transcription of genes with cAMP-responsive elements in their promoters [23, 26]. CREB is a component of intracellular signaling cascades that regulate a wide range of biological functions, from spermatogenesis to circadian rhythms and memory formation [11]. Increases in the concentration of either calcium or cAMP can trigger the phosphorylation and therefore the activation of CREB [14, 21]. Previous to our study, PRG-1 was identified as a potential target of the CREB regulon. On the one hand in a serial analysis of chromatin occupancy (SACO) library derived from rat PC12 cells [13], on the other hand in a genome-wide approach for characterization of target genes that are regulated by CREB in different cellular contexts [43]. Although CREB is a widely expressed transcription factor, it facilitates a variety of specific responses in the nervous system [19, 33]. Computer-aided analysis predicted a CpG island surrounding the CRE site on the identified minimal promoter, raising the possibility of CREB binding in vivo,

since CpG methylation interferes with CREB binding [12]. Besides the assumption of CREB governing the specific neuronal stimulation on the identified minimal promoter, alternatively, another binding site on this fragment mediates the neuronal specificity and CREB together with Sp1 amplify this transcriptional stimulation. Additionally, it is worth mentioning that PRG-1 and PRG-5, both expressed in brain and testis, are positioned on the same chromosome, in ≈300-kb distance, a feature conserved between human and rodents so they might share regulatory elements necessary for tissue-specific expression.

Members of the bHLH- transcription factor family are involved in vertebrate neurogenesis, depending on whether they act early or late during the differentiation process. They were designated as neuronal determination factors regulating competence or determination; the latter were termed as neuronal differentiation factors [10, 15, 16]. For example, Nex1 transcripts mark brain regions generally associated with learning and memory formation [3]. The spatial and temporal expression pattern of Nex1 overlaps with PRG-1 and thus includes the feature that expression is absent in GABAergic interneurons [9]. This, in turn, makes Nex1 an ideal candidate for conferring the strict neuronal expression of PRG-1. A recent study shows by chromatin immunoprecipitation assays that Nex1 binds directly to at least one E-Box in the promoter region of PRG-1 and that it also mediates neurite outgrowth via PRG-1 expression in PC12 cells [40]. The transcriptional stimulation of PRG-1 by the factor Nex1 via a specific E-Box motif in the rat sequence could be confirmed in our dual-luciferase assays in HEK 293 cells. For control purposes, we subcloned homologous murine and human sequences of this rat PRG-1 promoter sequence, in which Nex1 binding has been documented. These murine and human control vectors display similar enhancement of transcriptional stimulation, following Nex1 cotransfection. As the E-box motif at which Nex1 binding in rat was reported is not conserved in mouse and human sequences, potentially another adjacent E-box is responsible for the Nex1-mediated stimulation. However, fragments without any E-Box motifs (e.g., m−160/+145) displayed similar transcriptional activation to fragments with functional E-boxes after Nex1 cotransfection in HEK 293 cells. Another explanation could be that the regulation performed by Nex1 on the transcription of PRG-1 is not direct; and that a potential direct interaction partner needs to be identified in further studies. Nevertheless, our study documents a Nex1-dependent transcriptional stimulation of all tested deletion constructs.

To investigate at which step the basic helix-loop-helix (bHLH) transcription factor Nex1 is involved in the regulation of PRG-1 and to address the question whether Nex1 even drives the strictly neuronal expression of PRG-1, we analyzed subsequent PRG-1 expression on Nex1-null models. As Nex1-null mice are fully viable without obvious phenotypic alterations [29], Nex1 deficiency in vivo leads, as expected, to no detectable difference in PRG-1 expression regarding amount and location. These findings point to possible compensation between neuronal bHLH proteins, presumably accounting for this effect.

Our studies have determined a Nex1-independent regulation of PRG-1, which is mediated by a 450-bp promoter fragment that confers enhanced specific transcription in neurons. This regulation can be demonstrated under organotypic conditions, which underlines that this sequence is sufficient for the expression of PRG-1 in neurons. Further studies have to unravel the transcriptional regulators involved in this specific expression, which appears to be independent of Nex1.

Acknowledgments This work was supported by the DFG: SFB 665/B3 to R. Nitsch. Katja Becker and Boris Jerchow are acknowledged for their help with oocyte injection. The Nex1 null mutant was a kind gift of K.A. Nave, MPI for Experimental Medicine, Göttingen, Germany.

References

1. Banker G, Goslin K (1988) Developments in neuronal cell culture. Nature 336:185–186
2. Banker GA, Cowan WM (1977) Rat hippocampal neurons in dispersed cell culture. Brain Res 126:397–398
3. Bartholomä A, Nave KA (1994) NEX-1: a novel brain-specific helix-loop-helix protein with autoregulation and sustained expression in mature cortical neurons. Mech Dev 48:217–228
4. Bräuer AU, Nitsch R (2008) Plasticity-related genes (PRGs/LRPs): a brain-specific class of lysophospholipid-modifying proteins. Biochim Biophys Acta 1781:595–600
5. Bräuer AU, Savaskan NE, Kühn H, Prehn S, Ninnemann O, Nitsch R (2003) A new phospholipid phosphatase, PRG-1, is involved in axon growth and regenerative sprouting. Nat Neurosci 6:572–578
6. Brewer GJ, Torricelli JR, Evege EK, Price PJ (1993) Optimized survival of hippocampal neurons in B27-supplemented Neurobasal, a new serum-free medium combination. J Neurosci Res 35:567–576
7. Brindley DN (2004) Lipid phosphate phosphatases and related proteins: signaling functions in development, cell division, and cancer. J Cell Biochem 92:900–912
8. Brindley DN, Waggoner DW (1998) Mammalian lipid phosphate phosphohydrolases. J Biol Chem 273:24281–24284
9. Goebbels S, Bormuth I, Bode U, Hermanson O, Schwab MH, Nave KA (2006) Genetic targeting of principal neurons in neocortex and hippocampus of NEX-Cre mice. Genesis 44:611–621
10. Guillemot F (1999) Vertebrate bHLH genes and the determination of neuronal fates. Exp Cell Res 253:357–364
11. Habener JF, Miller CP, Vallejo M (1995) cAMP-dependent regulation of gene transcription by cAMP response element-binding protein and cAMP response element modulator. Vitam Horm 51:1–57
12. Iguchi-Ariga SM, Schaffner W (1989) CpG methylation of the cAMP-responsive enhancer/promoter sequence TGACGTCA abolishes specific factor binding as well as transcriptional activation. Genes Dev 3:612–619

13. Impey S, McCorkle SR, Cha-Molstad H, Dwyer JM, Yochum GS, Boss JM, McWeeney S, Dunn JJ, Mandel G, Goodman RH (2004) Defining the CREB regulon: a genome-wide analysis of transcription factor regulatory regions. Cell 119:1041–1054
14. Johannessen M, Delghandi MP, Moens U (2004) What turns CREB on? Cell Signal 16:1211–1227
15. Kageyama R, Ishibashi M, Takebayashi K, Tomita K (1997) bHLH transcription factors and mammalian neuronal differentiation. Int J Biochem Cell Biol 29:1389–1399
16. Lee JE (1997) Basic helix-loop-helix genes in neural development. Curr Opin Neurobiol 7:13–20
17. Lehnardt S, Henneke P, Lien E, Kasper DL, Volpe JJ, Bechmann I, Nitsch R, Webers JR, Golenbock DT, Vartanian T (2006) A mechanism for neurodegeneration induced by group B streptococci through activation of the TLR2/MyD88 pathway in Microglia1. J Immunol 177:583–592
18. Lin KI, Lee SH, Narayanan R, Baraban JM, Hardwick JM, Ratan RR (1995) Thiol agents and Bcl-2 identify an alphavirus-induced apoptotic pathway that requires activation of the transcription factor NF-kappa B. J Cell Biol 131:1149–1161
19. Lonze BE, Ginty DD (2002) Function and regulation of CREB family transcription factors in the nervous system. Neuron 35:605–623
20. Massari ME, Murre C (2000) Helix-loop-helix proteins: regulators of transcription in eucaryotic organisms. Mol Cell Biol 20:429–440
21. Mayr B, Montminy M (2001) Transcriptional regulation by the phosphorylation-dependent factor CREB. Nat Rev Mol Cell Biol 2:599–609
22. McDermott MI, Sigal YJ, Sciorra VA, Morris AJ (2004) Is PRG-1 a new lipid phosphatase? Nat Neurosci 7:789–790
23. Montminy MR, Sevarino KA, Wagner JA, Mandel G, Goodman RH (1986) Identification of a cyclic-AMP-responsive element within the rat somatostatin gene. Proc Natl Acad Sci USA 83:6682–6686
24. Novina CD, Roy AL (1996) Core promoters and transcriptional control. Trends Genet 12:351–355
25. Peeva GP, Angelova SK, Guntinas-Lichius O, Streppel M, Irintchev A, Schütz U, Popratiloff A, Savaskan NE, Bräuer AU, Alvanou A, Nitsch R, Angelov DN (2006) Improved outcome of facial nerve repair in rats is associated with enhanced regenerative response of motoneurons and augmented neocortical plasticity. Eur J Neurosci 8:2152–2162
26. Sassone-Corsi P (1995) Transcription factors responsive to cAMP. Annu Rev Cell Dev Biol 11:355–377
27. Savaskan NE, Bräuer AU, Nitsch R (2004) Molecular cloning and expression regulation of PRG-3, a new member of the plasticity-related gene family. Eur J Neurosci 1:212–220
28. Schwab MH, Bartholomae A, Heimrich B, Feldmeyer D, Druffel-Augustin S, Goebbels S, Naya FJ, Zhao S, Frotscher M, Tsai MJ, Nave KA (2000) Neuronal basic helix-loop-helix proteins (NEX and BETA2/Neuro D) regulate terminal granule cell differentiation in the hippocampus. J Neurosci 20:3714–3724
29. Schwab MH, Druffel-Augustin S, Gass P, Jung M, Klugmann M, Bartholomae A, Rossner MJ, Nave KA (1998) Neuronal basic helix-loop-helix proteins (NEX, neuroD, NDRF): spatiotemporal expression and targeted disruption of the NEX gene in transgenic mice. J Neurosci 18:1408–1418
30. Shimizu C, Akazawa C, Nakanishi S, Kageyama R (1995) MATH-2, a mammalian helix-loop-helix factor structurally related to the product of Drosophila proneural gene atonal, is specifically expressed in the nervous system. Eur J Biochem 229:239–248
31. Sigal YJ, McDermott MI, Morris AJ (2005) Integral membrane lipid phosphatases/phosphotransferases: common structure and diverse functions. Biochem J 387:281–293
32. Sigal YJ, Quintero OA, Cheney RE, Morris AJ (2007) Cdc42 and ARP2/3-independent regulation of filopodia by an integral membrane lipid-phosphatase-related protein. J Cell Sci 120:340–352
33. Silva AJ, Kogan JH, Frankland PW, Kida S (1998) CREB and memory. Annu Rev Neurosci 21:127–148
34. Trimbuch T, Beed P, Vogt J, Schuchmann S, Maier N, Kintscher M, Breustedt J, Schuelke M, Streu N, Kieselmann O, Brunk I, Laube G, Strauss U, Battefeld A, Wende H, Birchmeier C, Wiese S, Sendtner M, Kawabe H, Kishimoto-Suga M, Brose N, Baumgart J, Geist B, Aoki J, Savaskan NE, Bräuer AU, Chun J, Ninnemann O, Schmitz D, Nitsch R (2009) Synaptic PRG-1 modulates excitatory transmission via lipid phosphate-mediated signaling. Cell 138:1222–1235
35. Uesaka N, Hirai S, Maruyama T, Ruthazer ES, Yamamoto N (2005) Activity dependence of cortical axon branch formation: a morphological and electrophysiological study using organotypic slice cultures. J Neurosci 25:1–9
36. Uittenbogaard M, Baxter KK, Chiaramello A (2009) NeuroD6 genomic signature bridging neuronal differentiation to survival via the molecular chaperone network. J Neurosci Res 88:33–54
37. Uittenbogaard M, Chiaramello A (2002) Constitutive overexpression of the basic helix-loop-helix Nex1/MATH-2 transcription factor promotes neuronal differentiation of PC12 cells and neurite regeneration. J Neurosci Res 67:235–245
38. Uittenbogaard M, Chiaramello A (2004) Expression profiling upon Nex1/MATH-2-mediated neuritogenesis in PC12 cells and its implication in regeneration. J Neurochem 91:1332–1343
39. Wierstra I (2008) Sp1: emerging roles–beyond constitutive activation of TATA-less housekeeping genes. Biochem Biophys Res Commun 372:1–13
40. Yamada M, Shida Y, Takahashi K, Tanioka T, Nakano Y, Tobe T, Yamada M (2008) Prg1 is regulated by the basic helix-loop-helix transcription factor Math2. J Neurochem 106:2375–2384
41. Yamamoto N, Kurotani T, Toyama K (1989) Neural connections between the lateral geniculate nucleus and visual cortex in vitro. Science 245:192–194
42. Yamamoto N, Yamada K, Kurotani T, Toyama K (1992) Laminar specificity of extrinsic cortical connections studied in coculture preparations. Neuron 9:217–228
43. Zhang X, Odom DT, Koo SH, Conkright MD, Canettieri G, Best J, Chen H, Jenner R, Herbolsheimer E, Jacobsen E, Kadam S, Ecker JR, Emerson B, Hogenesch JB, Unterman T, Young RA, Montminy M (2005) Genome-wide analysis of cAMP-response element binding protein occupancy, phosphorylation, and target gene activation in human tissues. Proc Natl Acad Sci USA 102:4459–4464